

A First Principles Study of Carbon–Carbon Coupling over the {0001} Surfaces of Co and Ru

Q. Ge and M. Neurock*

Department of Chemical Engineering, University of Virginia, Charlottesville, Virginia 22903

H. A. Wright and N. Srinivasan

Refining Technology Group, Conoco Inc., 6592 Research West, 100 S. Pine, Ponca City, Oklahoma 74602-1267

Received: August 20, 2001; In Final Form: January 17, 2002

The coupling of CH (methyldiyne) and CH₂ (methylene), to form CHCH₂ (vinyl), over Co and Ru surfaces has been studied with the nonlocal gradient-corrected density functional theory slab calculations. The results show that this reaction is slightly exothermic on Co while endothermic on Ru within a (2 × 2) surface unit cell. Transition states were isolated on both surfaces, and the reaction barriers were found to be 55.9 and 116.5 kJ/mol on Co and Ru, respectively. The structures of the transition state on the two metal surfaces are similar; both involve the formation of a multicentered bond.

Fischer–Tropsch synthesis is a well-established catalytic process that converts syngas (CO and H₂) into hydrocarbons. The overall process is comprised of a network of the elementary bond-breaking and bond-formation steps. These include CO and H₂ activation as well as hydrogenation and chain growth over support metals. The balance of the bond-breaking and bond-formation processes on the metal surface dictates the choice of metal. Transition metals to the left in the periodic table will readily activate CO, but the products, i.e., surface carbon and oxygen, are too strongly bound to the surface thus blocking subsequent hydrogenation and carbon coupling reactions. Transition metals to the right, on the other hand, are not active enough to dissociate CO. The optimal metals are those which can promote CO activation, along with a balanced degree of surface hydrogenation and hydrocarbon coupling in order to produce longer chain hydrocarbon products.

Fischer–Tropsch has been analyzed in great detail since it was first discovered in the 1920s.¹ Most of the previous studies have focused on syntheses and characterization of different catalysts.² It is generally agreed that CO dissociation is the rate-limiting step and that the carbon chain growth involves the sequential insertion of CH₂ groups into the growing chain.³ Therefore, most of theoretical studies in the literature have been focused on the dissociation of CO and its subsequent hydrogenation to form C₁ hydrocarbons.⁴ Carbon–carbon coupling, however, is critical in chain growth and determines the ultimate product distribution. Despite its importance, there are only a handful theoretical analyses focused on carbon coupling; many of them are empirical or semiempirical.^{5,6} Using the tight binding extended Hückel method, Zheng et al. calculated the reaction energies and barriers for CH₃ + CH₃, CH₃ + CH₂, as well as CH₂ + CH₂ coupling reactions on Ti{0001}, Cr{110}, and Co{0001}.⁵ They found that the endothermicity decreases for CH₃ coupling with CH₃ or CH₂ across the periodic table from left to right. The barriers for the coupling reactions follow a similar

trend, whereas there is no barrier for CH₂ + CH₂ reaction on Co{0001}. Burghgraef et al. reported a density functional theory cluster calculation for the C–C coupling of C + CH, C + CH₂, as well as C + CH₃ on Ni and Co.⁶ In particular, they calculated the potential energy surface for C + CH₃ over Ni and Co with clusters of different sizes. The reaction was found to be exothermic on both surfaces. The activation energy and the overall reaction energy were found to be somewhat cluster size dependent. For a 13-atom Co cluster, they are +47 and –89 kJ/mol, respectively.

In the present study, we examine the coupling of chemisorbed methyldiyne and methylene intermediates over the Co{0001} and Ru{0001} surfaces. The reasons for choosing these systems are (1) both metals are industrially important Fischer–Tropsch catalysts, (2) both CH and CH₂ are important intermediates on the surface in the sequential chain growth processes, and (3) the product of this coupling reaction, an adsorbed vinylic species, can be a major intermediate in participating chain growth as a unit and leading to the formation of alkene.

All calculations described herein were performed within the framework of density functional theory (DFT) using a basis set consisting of plane waves, as implemented in the VASP code.⁷ The electron–ion interactions were described by ultrasoft pseudopotentials,⁸ and the exchange and correlation energies were calculated with the Perdew–Wang form of the generalized gradient approximation (GGA).⁹ Spin-polarization and nonlinear core corrections¹⁰ were included in the calculations for systems with Co to correctly account for its magnetic properties. Spin-polarization has been shown to have a major effect on the adsorption energies for magnetic systems¹¹ and may alter the topology of the potential energy surfaces.

Both Co and Ru are hexagonal close-packed metals, and the {0001} surface is the close-packed surface. In our calculations, the surface was modeled by a four-layer slab with a p(2 × 2) surface unit cell, as shown in Figure 1, separated by a vacuum region equivalent to six bulk metal layers. The one-sided slab has been used extensively in the literature and has been proven

* To whom correspondence should be addressed. Fax: 434 982 2658. E-mail: mn4n@virginia.edu.

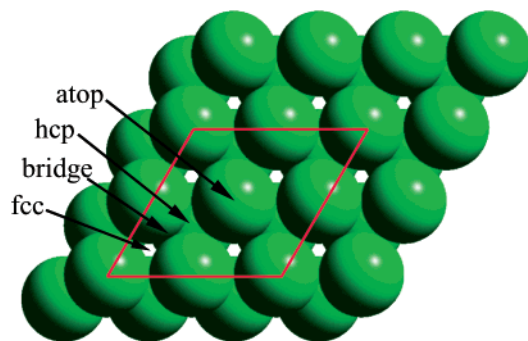


Figure 1. Schematic top view of the {0001} surface of Co and Ru. Shown also is the surface unit cell used in the calculations and the high-symmetry sites referred to in the text.

to be accurate.^{12,13} A plane wave cutoff energy of 280 eV was used in the calculation, and the Brillouin zone of the surface unit cell was sampled with a 5×5 Monkhorst–Pack mesh.¹⁴ Convergence tests have been performed by increasing the cutoff energy to 320 eV and the k-point mesh to 7×7 . The changes in the calculated adsorption structures and energies are negligible. The metal atoms in the bottom two layers were fixed at their bulk positions, whereas the atoms in the top two layers and the hydrocarbon adsorbates were allowed to relax. A conjugate-gradient minimization scheme or a quasi-Newton method was used for ionic geometry optimization. Transition states were isolated by using the nudged-elastic band method that is implemented in VASP.¹⁵

We first calculated the adsorption structures and energetics of methylidyne, methylene, and vinyl on the surfaces to establish the reactant and product states for the C–C coupling reaction of CH and CH₂. All of the reported adsorption energies were calculated by taking the difference between the total adsorbate/surface system and the individual surface and individual adsorbate:

$$\Delta E_{\text{ads}} = E_{\text{ADS/surface}} - E_{\text{ADS}} - E_{\text{surface}}$$

Herein we used the experimental convention that the heat of adsorption is reported as a positive number, i.e.

$$Q = -\Delta E_{\text{ads}}$$

Methylidyne is the most strongly bonded C₁ hydrocarbon on metal surfaces. On the close-packed surfaces, it prefers to sit in the hollow sites. On both Co and Ru, our results show hcp hollow sites to be the most favorable sites, with adsorption energies of 623.5 and 660.9 kJ/mol, respectively, with respect to a gas phase methylidyne in the most stable doublet state. Methylidyne in the fcc hollow sites is less stable than that in the hcp sites, with adsorption energies of 604.7 and 628.7 kJ/mol on Co and Ru, respectively. These results agree with that of Ciobica et al., who report that methylidyne is most strongly bound to the hcp hollow site on Ru.¹⁶ Figure 2a shows a schematic view of CH adsorbed in a hcp hollow site. The structural parameters along with the calculated binding energies of the adsorbed methylidyne in all of the sites examined are collected in Table 1.

Methylene is one of the active intermediates added on as a unit during chain growth process in Fischer–Tropsch synthesis. From a geometrical consideration, the bridge sites are expected to be the most stable adsorption sites for CH₂ as the two bridging metal atoms and the H atoms in CH₂ lead to the ideal tetrahedral structure for an sp³ hybridized carbon. The adsorption energies in the bridge site on Co and Ru are 360.2 and 389.1 kJ/mol,

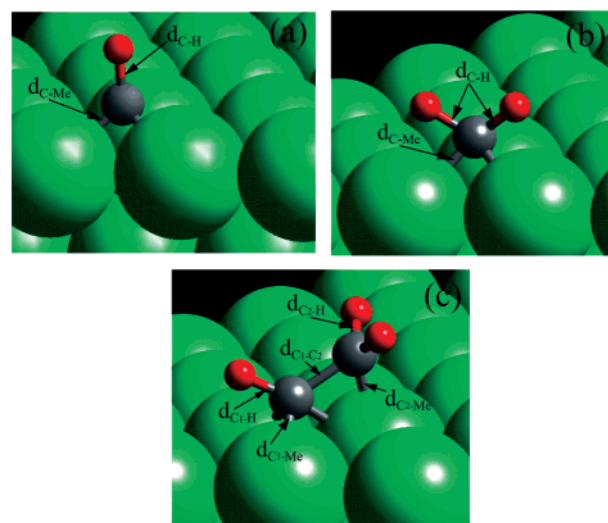


Figure 2. Schematic views of (a) CH, (b) CH₂, and (c) vinyl adsorbed in their most stable adsorption sites (hcp site) on Co and Ru surfaces. Large green spheres, Co or Ru surface atoms; red spheres, H atoms; dark gray spheres, C atoms. The structural parameters are given in Tables 1–3.

TABLE 1: DFT-GGA Calculated Adsorption Energies (E_b) and Structures for Methylidyne (CH) on Co{0001} and Ru{0001}^a

	Co			Ru	
	bridge	fcc	hcp	fcc	hcp
E_b (kJ/mol)	592.1	604.7	623.5	628.8	660.9
$d_{\text{C-Me}}$ (Å)	1.817	1.880	1.879	2.040	2.042
$d_{\text{C-H}}$ (Å)	1.102	1.099	1.103	1.096	1.096

^a All adsorption energies, E_b , refer to the relaxed clean surface and CH in the doublet state; $d_{\text{C-Me}}$ and $d_{\text{C-H}}$ are the C–metal and C–H bond lengths, respectively.

TABLE 2: DFT-GGA Adsorption Energies (E_b) and Structures for Methylene (CH₂) on Co{0001} and Ru{0001}^a

	Co				Ru	
	bridge1 ^b	bridge2 ^c	fcc	hcp	bridge2	hcp
E_b (kJ/mol)	351.7	360.0	377.2	384.1	389.1	412.4
$d_{\text{C-Me}}$ (Å)	1.905	1.939	1.988	1.981	2.086	2.130
$d_{\text{C-H}}$ (Å)	1.113	1.107	1.113	1.114	1.107	1.120
$\angle\text{HCH}$ (deg)	107.1	107.1	106.7	106.5	107.0	104.7

^a All adsorption energies, E_b , refer to the relaxed clean surface and CH₂ in the triplet state; $d_{\text{C-Me}}$ and $d_{\text{C-H}}$ are referred to C–metal and C–H bond lengths, respectively. ^b bridge1: HCH plane is in the same plane as the bridging metal atoms. ^c bridge2: HCH plane is perpendicular to the bridging atoms.

respectively. However, our results show that the hcp hollow site is the energetically most favorable site, by 24.1 and 23.3 kJ/mol on Co and on Ru, respectively, more than that of the bridge site. The results for methylene on Ru{0001} are also consistent with the reported results by Ciobica et al.¹⁶ A schematic view of CH₂ in a hcp hollow site is shown in Figure 2b. The structural parameters of the adsorbed CH₂ species on Co and Ru are listed in Table 2.

Vinyl is the direct product of the CH + CH₂ coupling reaction and is a basic step in carbon chain growth in Fischer–Tropsch synthesis.¹⁷ Although vinyl has not been isolated cleanly on single-crystal surfaces,¹⁸ it was suggested as an important intermediate for initiating chain growth based on the experimental results using isotope labeling.¹⁹ Our calculation results show that vinyl prefers hcp hollow sites, in which the C atoms of CH end point to the hollow site, whereas the other C atom

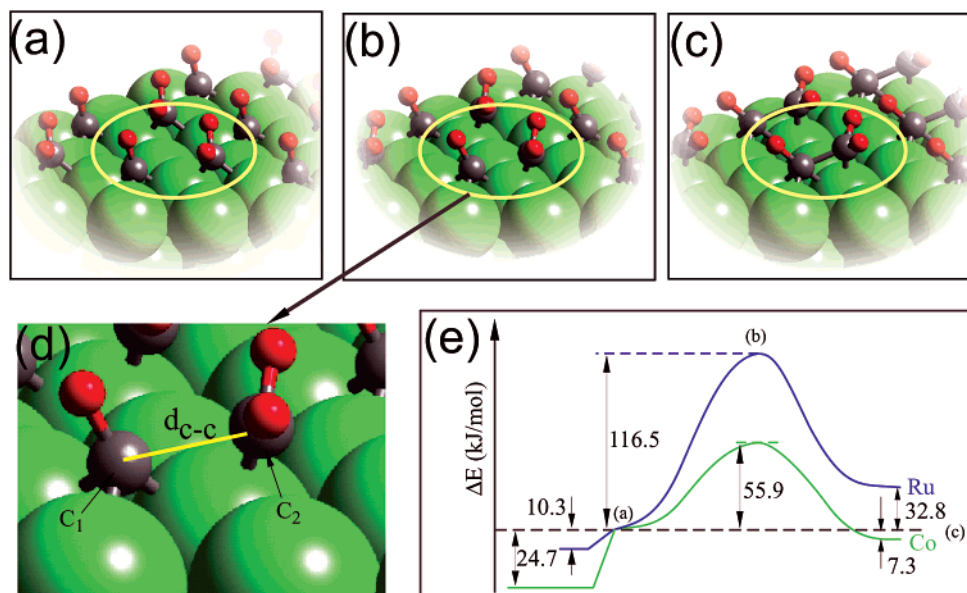


Figure 3. Images of reactant state (a), transition state (b), and product state (c) of C–C coupling reactions in a (2×2) surface unit cell on Co{0001} and Ru{0001}. An enlarged image of the transition state is shown in d, and the structural parameters are given in Table 4. Schematic potential energy surfaces from state a to c via transition state b on both Co and Ru are shown in e.

is close to the atop site. In the adsorbed vinyl, the C–C bond is significantly tilted, by $\sim 30^\circ$ off the surface plane. Figure 2c shows the structure of vinyl chemisorbed in an hcp hollow site. The adsorption energies for vinyl are 228.3 and 275.7 kJ/mol for Co and Ru, respectively. The structural parameters for adsorbed vinyl are listed in Table 3. The CH carbon of vinyl is effectively bonded to three surface metal atoms. The bond length of the third M–C bond is only about 0.15 Å longer than the other two M–C bonds.

To study the C–C coupling reaction, we calculated CH and CH₂ coadsorbed in the (2×2) unit cell. These two species share one metal atom and repel each other when they are coadsorbed in a (2×2) surface unit cell. The repulsive interaction energies are 24.7 and 10.3 kJ/mol on Co and Ru, respectively. These interaction energies represent the energy cost to move CH and CH₂ from their isolated sites on the surface to the positions for reaction to proceed. The symmetrical structures found for the pure adsorbate layer are distorted when they are coadsorbed. With respect to the coadsorbed CH and CH₂, the reaction energies are -7.3 and $+32.8$ kJ/mol on Co and Ru, respectively. However, the overall CH + CH₂ reaction would be endothermic on both Co and Ru if the repulsive interaction energy between CH and CH₂ is taken into account. The overall reaction energies become 17.4 and 43.1 kJ/mol on Co and Ru, respectively. This indicates that the C–C coupling reaction of CH with CH₂ is not favored on either of the surfaces at lower coverages.

After establishing the structures of the reactants, coadsorbed CH and CH₂ in the adjacent hcp sites, and of the product, vinyl, we then proceed to search for the transition state. A series of images are interpolated between the reactant state and product to establish the linear transient reaction path. The structure for each of these images is optimized subjected to the constraint that movements are only allowed along the directions perpendicular to the hyp tangent, as outlined in the nudged elastic band method.¹⁵ In Figure 3a–c, we show the images of reactant state (a), transition state (b), and product state (c) for the reaction on Co. As the calculation has been done with a periodic unit cell, one should focus their attention on the pair shown inside the yellow oval in the figure. An enlarged image of the transition

TABLE 3: DFT-GGA Adsorption Energies and Structures for Vinyl (CHCH₂) on Co{0001} and Ru{0001}^a

	Co		Ru hcp
	fcc	hcp	
E_b (kJ/mol)	217.8	228.3	275.7
d_{C-C} (Å)	1.448	1.448	1.454
d_{C_1-Me} (Å)	1.969	1.973	2.110
d_{C_1-H} (Å)	1.115	1.117	1.121
d_{C_2-Me} (Å)	2.021	2.013	2.148
d_{C_2-H} (Å)	1.096	1.097	1.096

^a All adsorption energies, E_b , refer to the relaxed clean surface and CHCH₂ in the doublet state.

TABLE 4: Transition State Structures for C–C Coupling Reaction of CH and CH₂ on Co{0001} and Ru{0001}

	Co	Ru	
		path 1	path 2
d_{C-C} (Å)	1.899	1.976	2.019
d_{C_1-Me} (Å)	1.883, 2.088, 1.920	2.088, 2.117, 2.043	2.082, 2.082, 2.057
d_{C_1-H} (Å)	1.099	1.099	1.098
d_{C_2-Me} (Å)	1.901, 2.364, 2.478	2.005, 2.815, 2.895	1.990, 2.896, 3.142
d_{C_2-H} (Å)	1.110	1.097	1.094

state is shown in Figure 3d. The C–C distances at this transition state are 1.93 and 2.01 Å on Co and Ru, respectively. The detailed structural parameters of the transition states on Co and on Ru are shown in Table 4. Schematics of the reaction energetics on both surfaces are shown in Figure 3e. The activation barriers for the coupling reactions on Co and Ru are 55.9 and 116.5 kJ/mol, respectively. For the reaction on Ru{0001}, we examined two different starting geometries: CH₂ from the most stable hcp site (path 1) and from the bridge site (path 2). The structures of the transition state for these two paths are very similar.

As shown in Table 4, the structures of the transition state are very similar on both surfaces. The key differences are the specific bond lengths. Generally, the bond distances are longer on Ru than on Co, and this is in accord with the fact that the lattice constant of Ru are longer than that of Co. This is also one of the reasons that the repulsive interaction energy between the reactants, CH and CH₂, is smaller on Ru than on Co. At

this state, two (one for path 2) of the C–metal bonds of the initial adsorbed CH₂ are broken, and the remaining one bond is shortened slightly. CH₂ is moved closer to CH, but the C–C distances are in the range from 1.90 to 2.02 Å on Co and Ru with different paths. The process to reach this transition state involves the activation of CH from its most stable hcp hollow site as the CH group begins to move and partial scission of C–M bond(s) of CH₂ in order to react with the activated CH.

The Evans–Polanyi relationship, which is an empirical linear relationship between the activation energy and the reaction energy for an elementary reaction, can be used to correlate the overall reaction energy to the activation energy. It has been widely used in heterogeneous catalysis to correlate the activation energies with the overall reaction energies for a series of reactions with structurally similar reactants.²⁰ This relationship has been quantified using DFT-based quantum chemical methods by Pallassana and Neurock²¹ and more recently by Nørskov's group.²² Pallassana and Neurock showed that the calculated barriers of the C–H bond activation on the Pd overlayer on different substrates linearly correlate with the exothermicity of the reaction.²¹ For the present C–C coupling reaction of CH and CH₂, the overall reaction would be endothermic at low coverages, as shown above. Only when the coverage is high enough, i.e., CH and CH₂ are pushed into the neighboring hollow sites, the reaction becomes slightly exothermic on Co. The change of the activation energy from Co to Ru correlates with the change of the reaction energy: the activation barrier is increased by ~60 kJ/mol, whereas the reaction energy is increased by ~40 kJ/mol.

The present results also indicate that the reverse process, the C–C activation of adsorbed vinyl species, is an exothermic process if the surface coverage is sufficiently low. Particularly, the C–C activation process is more favorable on Ru surface than on Co. This is consistent with the experimental observations that no vinyl is isolated under the ultrahigh vacuum condition on Ru.¹⁸ However, we note that the barrier for this activation is slightly lower on Co than that on Ru.

The coupling of CH and CH₂ surface fragments proceeds via a classic oxidative addition mechanism. The reaction proceeds via the migration of the adsorbed CH₂ toward the CH group to overcome the repulsive interactions between them. This occurs very early along the reaction channel. The change in the C–C bond length is relatively small as compared to its change from reactant to product. Both bonding (σ) and antibonding (σ^*) states begin to appear “early” along the reaction path. The bonding σ_{C-C} state shifts downward by –0.7 eV from the reactant to the transition state, whereas the antibonding σ^*_{C-C} state shifts upward by +0.2 eV. The shifts of both σ and σ^* states, however, are much greater (–1.1 eV for σ_{C-C} and +0.6 eV for σ^*_{C-C}) in moving from the transition state to the product state. This is because C–C bond formation occurs “early” along the reaction channel. Therefore, one would expect larger changes from the

transition state to the product than from the reactant state to the transition state. A detailed mechanistic analysis of the CH and CH₂ coupling process as well as the coupling of other possible surface CH_x fragments will be presented elsewhere.²³ The implication of the coupling reactions to the overall Fischer–Tropsch chemistry will also be examined.²³

The coupling of CH and CH₂ surface fragments can occur over the close packed surface of Co and Ru. Gradient-corrected periodic DFT calculations indicate that the reaction when carried out in a (2 × 2) surface unit cell is slightly exothermic on Co but endothermic on Ru, by –7.3 and +32.8 kJ/mol, respectively. The calculated barriers for the coupling reaction are 55.9 kJ/mol on Co and 116.5 kJ/mol on Ru. The higher barrier on Ru is consistent with the fact that the CH and CH₂ reactants bind more strongly on Ru than on Co.

Acknowledgment. The authors acknowledge Conoco, Inc., for their generous support of this work. A portion of the calculation has been carried out on the centurion nodes at the University of Virginia.

References and Notes

- (1) Fischer, F.; Tropsch, H. *Brennst. Chem.* **1923**, 4, 276; **1926**, 7, 97; *Chem. Ber.* **1926**, 59, 830.
- (2) Van der Laan, G. P.; Beenacker, A. A. C. M. *Catal. Rev.—Sci. Eng.* **1999**, 41, 255.
- (3) Thomas, J. M.; Thomas, W. J. *Principles and Practice of Heterogeneous Catalysis*; VCH: Weinheim (FRG), 1997; p 524.
- (4) Neurock, M. *Top. Catal.* **1999**, 9, 135.
- (5) Zheng, C.; Apeloig, Y.; Hoffmann, R. *J. Am. Chem. Soc.* **1988**, 110, 749.
- (6) Burghgraef, H.; Jansen, A. P. J.; van Santen, R. A. *J. Chem. Phys.* **1995**, 103, 6562.
- (7) (a) Kresse, G.; Hafner, J. *Phys. Rev. B* **1993**, 47, 558. (b) Kresse, G.; Furthmüller, J. *Phys. Rev. B* **1996**, 54, 11169. (c) Kresse, G.; Furthmüller, J. *Comput. Mater. Sci.* **1996**, 6, 15.
- (8) Vanderbilt, D. *Phys. Rev. B* **1990**, 41, 7892.
- (9) Perdew, J.; Chevary, J. A.; Vosko, S. H.; Jackson, K. A.; Pederson, M. R.; Singh, D. J.; Fiolhais, C. *Phys. Rev. B* **1992**, 46, 6671.
- (10) Louie, S. G.; Froyen, S.; Cohen, M. L. *Phys. Rev. B* **1982**, 26, 1738.
- (11) Ge, Q.; Jenkins, S. S.; King, D. A. *Chem. Phys. Lett.* **2000**, 327, 125.
- (12) Hammer, B.; Nørskov, J. K. *Adv. Catal.* **2000**, 45, 71.
- (13) Ge, Q.; Kose, R.; King, D. A. *Adv. Catal.* **2000**, 45, 207.
- (14) Monkhorst, H. J.; Pack, J. D. *Phys. Rev. B* **1976**, 13, 5188.
- (15) Mills, G.; Jónsson, H.; Schenter, G. K. *Surf. Sci.* **1995**, 324, 305.
- (16) Ciobica, I. M.; Frechard, F.; van Santen, R. A.; Kleyn, A. W.; Hafner, J. *Chem. Phys. Lett.* **1999**, 311, 185.
- (17) Bent, B. E. *Chem. Rev.* **1996**, 96, 1361.
- (18) Wu, M.-C.; Goodman, D. W.; Zajac, G. W. *Catal. Lett.* **1994**, 24, 23.
- (19) Wu, M.-C.; Goodman, D. W. *J. Am. Chem. Soc.* **1994**, 116, 1364.
- (20) Maitlis, P. M.; Long, H. C.; Quyoum, R.; Turner, M. L.; Wang, Z.-Q. *Chem. Commun.* **1996**, 1. Long, H. C.; Turner, M. L.; Fornasiero, P.; Kaspar, J.; Graziani, M.; Maitlis, P. M. *J. Catal.* **1997**, 167, 172.
- (21) Gates, B. C. *Catalytic Chemistry*; John Wiley & Sons: New York, 1992.
- (22) Pallassana, V.; Neurock, M. *J. Catal.* **2000**, 191, 301.
- (23) Logadottir, A.; Rod, T. H.; Nørskov, J. K.; Hammer, B.; Dahl, S.; Jacobsen, C. J. H. *J. Catal.* **2001**, 197, 229.
- (24) Ge, Q.; Neurock, M. To be submitted.